A qualitative analysis of Laser - Electron bunch interaction using ASTRA

Margarit Asatrian, Yerevan State University, Armenia

September 17, 2019

Supervisors: Klaus Floettmann, Benno Zeitler

Abstract

The report presents a qualitative analysis of the laser pulse - electron bunch interaction. The analysis is based on ASTRA simulations for a Gaussian laser beam and a low-energy relativistic electron bunch. Axially symmetrical, antisymmetrical and asymmetrical effects are discussed separately.

Contents

1 The overtaking problem

A high power laser pulse propagating in plasma creates a wakefield, which can be used to accelerate charged particles. The particles to be accelerated can be either taken directly from plasma (so-called internal injection) or injected externally. In the latter case, the particle bunch has to enter plasma shortly after the laser pulse: the phase offset has to be on the order of the plasma wavelength ($\sim 100 \mu m$). Before that, the laser pulse and the particle bunch travel collinearly in vacuum.

In our case, electrons are considered, which, though being relativistic, move slower than the photons, with $\beta = v/c = 0.9965$. In order to achieve the desired phase offset on the target, the laser pulse has to enter the co-propagation region with a corresponding time delay. That means that, at some point during the co-propagation, the electron bunch is overtaken by the laser pulse.

In the experiment, a well-known electron bunch has to be injected into plasma. Knowing the initial and final parameters of the bunch and the laser pulse, one can potentially reconstruct the processes, occurring in plasma. This, obviously, requires a high quality bunch.

For the electron bunch at REGAE (the Relativistic Electron Gun for Atomic Exploration), which typically has $\gamma \approx 12$, the overtaking happens at a distance of a few centimetres to the target. The laser is focused roughly in the middle of the plasma region, so the electron bunch meets a high intensity field near the focus (see [1]). Such an interaction can potentially spoil the quality of the bunch, which, as already mentioned, is crucial for the experiment.

2 ASTRA simulations

2.1 Overview

In [1] it was already shown, that the injection of the bunch is possible. In this project, mainly the worst-case-scenario is considered with the aim to get a deeper understanding of the overtaking process.

For the analysis, simulations were done with ASTRA (A Space Charge Tracking Algorithm), using the Gaussian laser beam description, implemented into the programme.

The laser pulse has a Gaussian transverse profile and a temporal profile, given by the hyperbolic secant. The electric field is polarised in the x direction (for the exact field description, see 6.14, [2])

In order to analyse purely the laser effect, an electron bunch with 0 initial emittance was chosen. The bunch has a Gaussian spatial distribution. The space charge forces are not included into the simulations.

Even in this idealised case the problem is complex, as various factors affect the behaviour of the electron bunch in a laser field.

The first effect to be considered is the ponderomotive force (F_p), caused by the inhomogeneity of the oscillating fields. During a part of the oscillation period, the particles,

Table 1: Laser Parameters

Parameter	Symbol	Value	Unit
Peak normalised vector potential	a_0	1.5	
Temporal $1/e$ of the laser field	τ	8.5E-14	s
Pulse energy	W	5.0	J
Wavelength	λ	8.2E-07	m
Beam waist	w_0	2.7E-05	m

Table 2: Electron bunch parameters

Parameter	Symbol	Value	Unit
Average energy	W_e	5.6	MeV
RMS size of the longitudinal distribution	σ_z	25E-4	mm
RMS size of the transverse distribution	σ_x,σ_y	15E-4	mm

being in the region with a stronger field, experience a greater force. This effect is not fully compensated in the weaker field, leading to a net drift towards the lower intensity region. This intuitive explanation is only valid for the direction of the electric field, while for the other transverse component, a coupling to the longitudinal field is required. The force depends on the magnitude and the gradient of the laser intensity and for a non-relativistic electron is given by

$$\mathbf{F_p} = -\frac{m_e c^2}{2}\nabla a^2.$$

It is important to consider also the laser evolution: the laser field is different on different longitudinal positions, having the highest intensity on focus. The strength of the effect is described by the Rayleigh length (Z_R) — the distance along the propagation direction of a beam from the waist to the place, where the laser spot size is doubled. For a Gaussian beam

$$Z_R = \frac{\pi w_0^2}{\lambda}.$$

In our case the Rayleigh length is about 2.72E-3 m (see $w0$ and λ in Table 1), so the overtaking process takes place over several Rayleigh lengths, which means that the laser field changes considerably during the overtaking. This puts an additional effect on the evolution of the longitudinal parameters of the bunch.

Finally, having fixed the initial parameters of the electron bunch and the laser pulse, the effect on the bunch depends strongly on the point, where the overtaking happens,

Table 3: Other parameters

Parameter	Symbol	Value	Unit
Initial longitudinal position	z_0	0.0	m
Longitudinal position of the laser focus	z_F	0.4	m
Longitudinal position of the final screen		0.5	m
Initial time delay of the laser	t		ns
Initial time delay of the laser in Run 1	t_0	4.2E-3	ns
Time step (difference in t between the runs)	Δt	2.5E-5	ns
Distance from the overtaking point to the laser focus	Δz		m

more precisely, on its distance from the laser focus. Of course, the overtaking process has a certain length, so we will consider the centre point of that interval. A scan of the initial delay (t) of the laser was performed, shifting the overtaking point. t was changed with a step Δt, starting from t_0.

For a given Δt, the distance from the overtaking point to the laser focus can be calculated by

$$\Delta z = \frac{c\beta\Delta t}{1-\beta} - z_F.$$

Δz will be mentioned along with the run number.

2.2 Symmetry of the problem

Both electron bunch and laser intensity distributions are axially symmetrical. Also, no transverse offset is introduced. Any kind of asymmetry will be caused by the polarisation of the laser. It should, though, have no net effect on the ponderomotive force, as it only depends on the intensity distribution.

Therefore, a certain degree of symmetry is expected; next chapters give a quick description of axially symmetrical, antisymmetrical and asymmetrical effects.

2.3 Symmetrical effects

The first parameter to be looked at is the transverse emittance (ϵ) of the bunch. On Fig. 1a, the black and red curves represent ϵ_x and ϵ_y. If the overtaking happens far enough from the focus ($\Delta z_1 \approx -0.043$), only a peak in ϵ_x can be seen, while ϵ_y is almost unaltered. The peak in ϵ_x is due to rapid oscillations, caused by the transverse electric field. After the interaction, the emittance (almost) comes back to the initial value. The bunch is slightly diverging, as it can be seen from Fig.1b .

As the overtaking point is shifted closer to the focus ($\Delta z_{13} \approx -0.018$), the final divergence and the transverse emittance increase. It can be seen how ϵ_y grows accordingly,

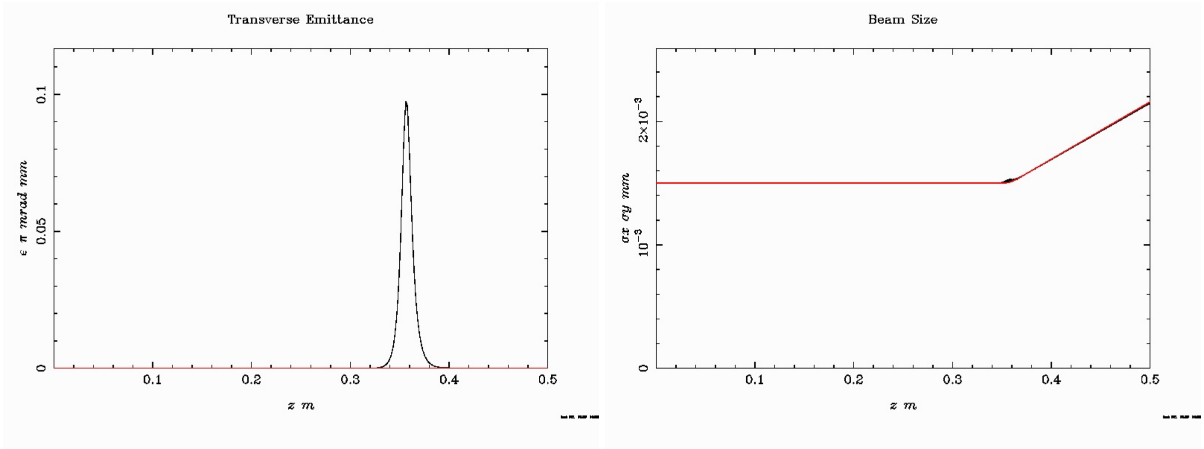

(a) Transverse emittance; ϵ_x (black) and ϵ_y (red)

(b) Rms beam size; σ_x (black) and σ_y (red)

Figure 1: Run 1, $\Delta z_1 \approx -0.043$

almost matching ϵ_x after the interaction (Fig. 2a). The same is true for the divergence (Fig. 2b).

We are, though, are limited by the fact that the beam has no initial divergence. For comparison, the result of another simulation is shown in Fig. 3 (the parameters are slightly altered, but that does not affect the overall picture). In this case, the electron bunch has an initial divergence, and it can be seen how in reality the divergence drops in one plane while rising in the other.

Coming back to the 0 emittance bunch, it is interesting to see how the longitudinal shape of the bunch evolves. The correlated energy spread is shown below on Fig. 4a. Judging by the sign of the function, one can see that during the overtaking, the bunch is compressed first, then stretched, then compressed again and stretched far after the interaction. This behaviour is explained by the ponderomotive force and the laser evolution. First, the bunch is hit by the falling intensity slope of the pulse; the tail sees a stronger force, what results in bunch compression. As the pulse propagates though the bunch, the tail and the head see respectively the rising and falling slopes of the intensity distribution, what stretches the bunch. As the pulse propagates further, the particles are affected by the falling slope, the head seeing a stronger field. Thus, the bunch is compressed again.

The above-described effects are only due to the ponderomotive force, but the intensity distribution itself changes during the overtaking. As the bunch is approaching the laser focus, every consecutive effect is stronger than the previous one and the bunch is compressed in the end. (The exact opposite behaviour is expected when the overtaking takes place after the focus.) After the interaction, the faster particles end up being in the tail, what results, in the end, in the rearrangement of the particles, and the bunch length increases again (Fig. 4b).

As the overtaking point approaches the focus ($\Delta z_{16} \approx 0.011$), it can be clearly seen, that the emittance does not remain constant after the interaction, which is due to the

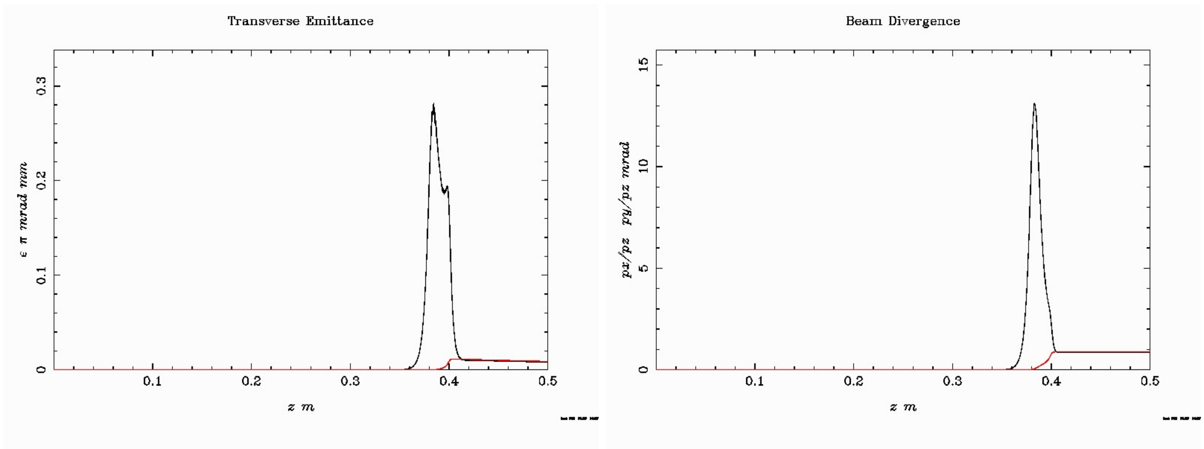

(a) Transverse emittance

(b) Rms beam divergence

Figure 2: Run 13, $\Delta z_{13} \approx -0.018$

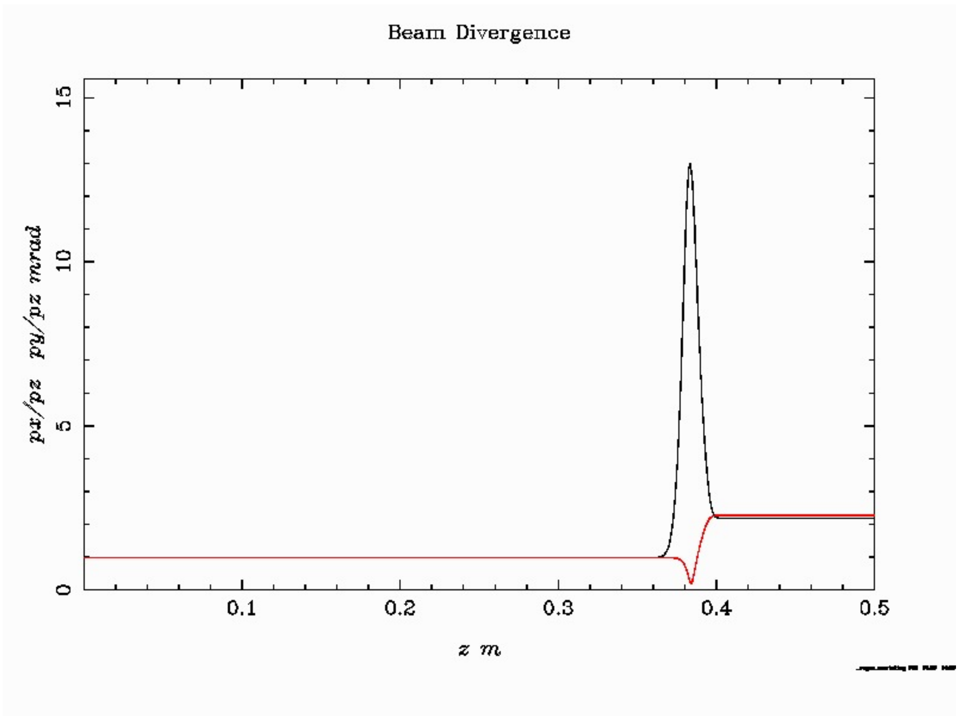

Figure 3: Rms beam divergence of a bunch with a non-zero initial emittance

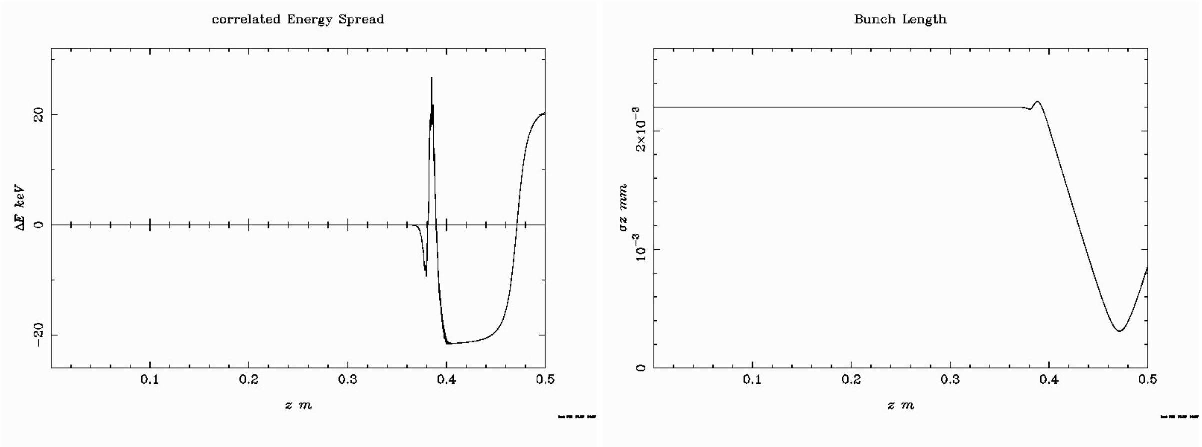

(a) Correlated energy spread

(b) Bunch length

Figure 4: Run 13

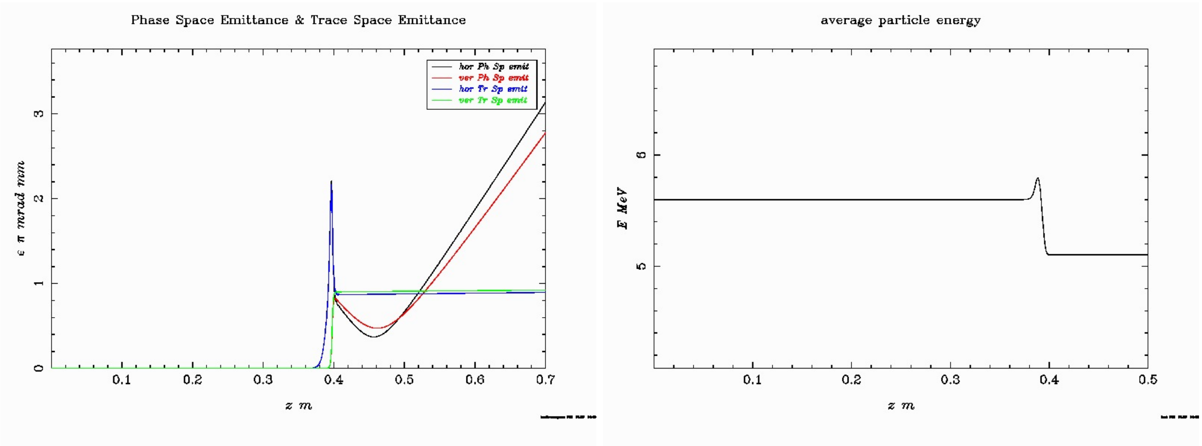

(a) Phase space and trace space emittance

(b) Average particle energy

Figure 5: Run 16, $\Delta z_{16} \approx -0.011$

energy spread and the divergence. Different transverse slices of the bunch have different energies, which means, that their corresponding ellipses in the phase space rotate with different velocities, so that the projection changes. The trace space emittance stays constant after the overtaking (Fig. 5a). Besides, the average energy falls after the interaction (Fig. 5b), which was also true for the previous cases, although the effect was smaller.

In the next case ($\Delta z_{20} \approx -0.003$), the average energy grows with respect to the initial value and the emittance rises dramatically, as shown on Figures 6b and 6a.

The divergence has been growing through all the above presented cases.

After Run 21 ($\Delta z_{21} \approx -0.0009$), the divergence starts to decrease, as the overtaking point shifts to the other side of the laser focus.

Eventually, the effects on the electron bunch get milder and the correlated energy

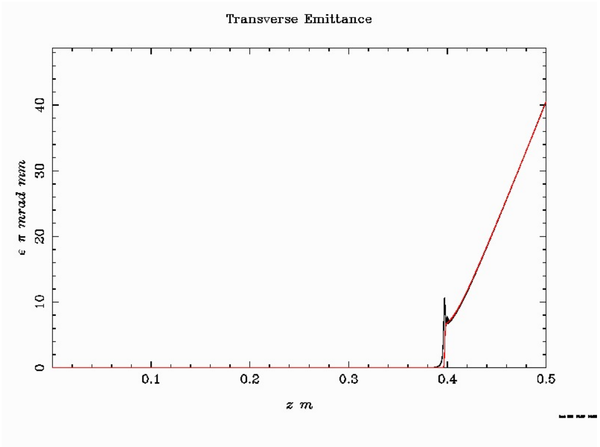

(a) Transverse emittance

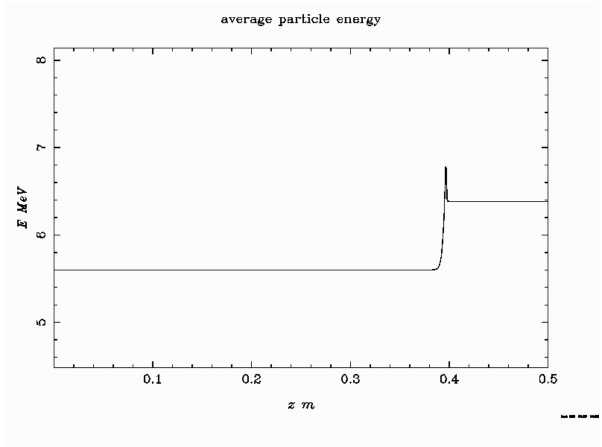

(b) Average particle energy

Figure 6: Run 20, $\Delta z_{20} \approx -0.003$

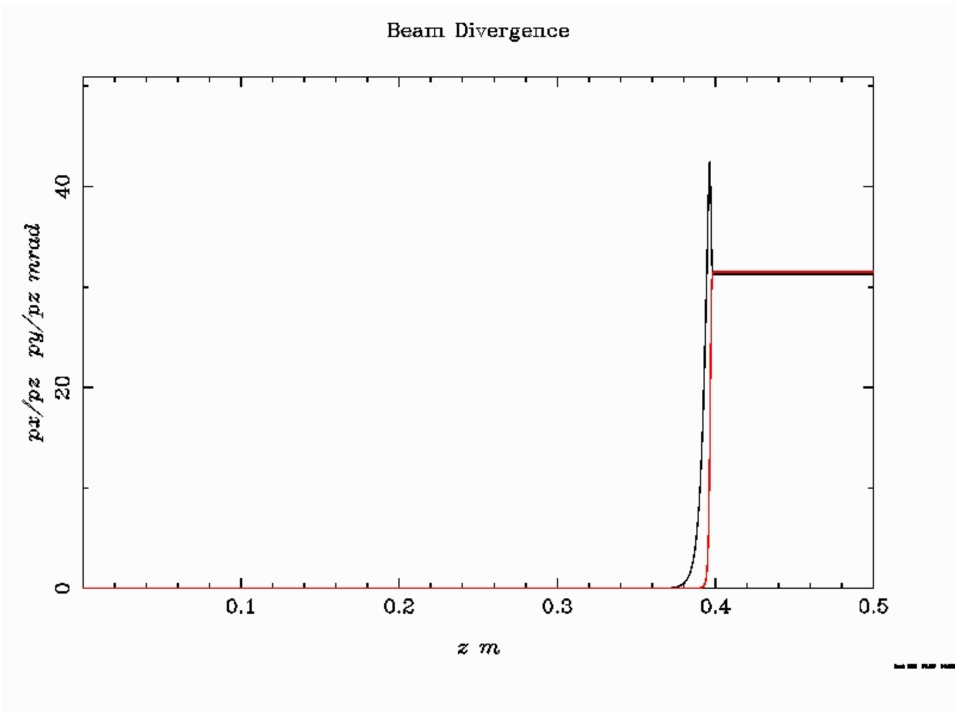

Figure 7: Run 20: Rms beam divergence

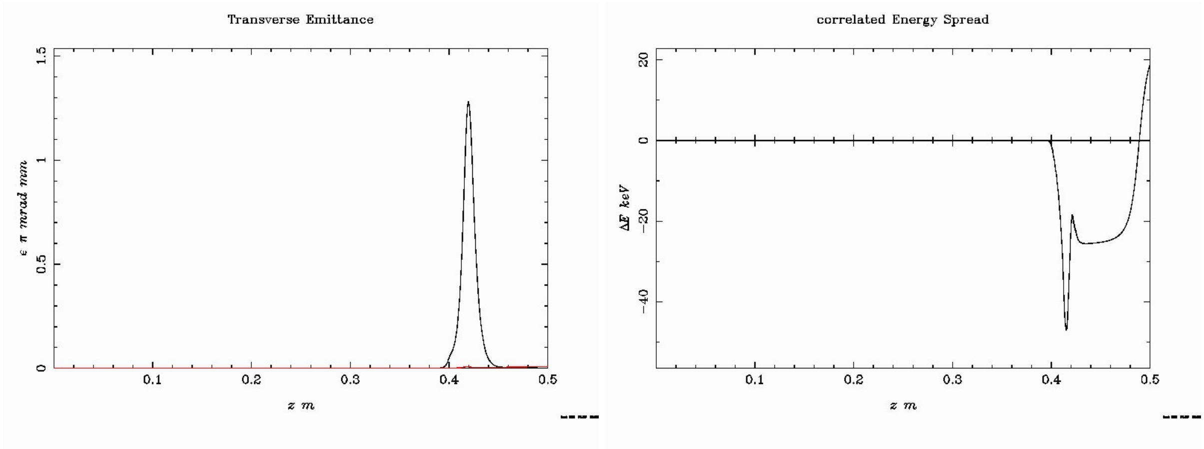

(a) Transverse emittance (b) Correlated energy spread

Figure 8: Run 30, $\Delta z_{30} \approx 0.018$

spread changes its behaviour, indicating that the overtaking point has fully passed the laser focus (Fig. 8b).

As expected, the correlated energy spread behaves in the opposite way, compared to the case, in which the overtaking takes place before the focus (see Fig. 4a). With the further shift of the overtaking point, the intensity of the laser - electron bunch interaction goes down, converging to zero.

It can be seen, that the difference of the final and initial average energies actually changes the sign (compare Figures 5b and 6b). The dependence of that difference on the run number (on the overtaking point) is shown in Fig.10. It should be noted, that the energy change is possible due to laser evolution.

2.4 Antisymmetrical effects

As stated above, the problem is not fully symmetrical, as the laser is polarised in the x direction. Certain asymmetry and antisymmetry can be found in the bunch distributions. For each of the above described cases the full particle distribution at several longitudinal positions was saved.

When shifting the overtaking point towards the focus, at some moment the particles start forming antisymmetrical crescent-like distributions in the $x-z$, $y-z$ planes (the particles are observed at $z=0.5$, 0.1 metres downstream the focus).

The particle distribution for Run 20 is shown in Fig. 11.

The projection on the transverse plane is a ring, which is the effect of the transverse ponderomotive force. The asymmetry in the longitudinal shape, however, cannot be explained in the same way.

To get a better understanding of the way the crescents are formed, the initial distribution was divided into five parts, depending on the longitudinal position. These five sub-ensembles were plotted separately. The plots below indicate that there is not much shuffling happening: the particles that were initially in the front, remained in the front

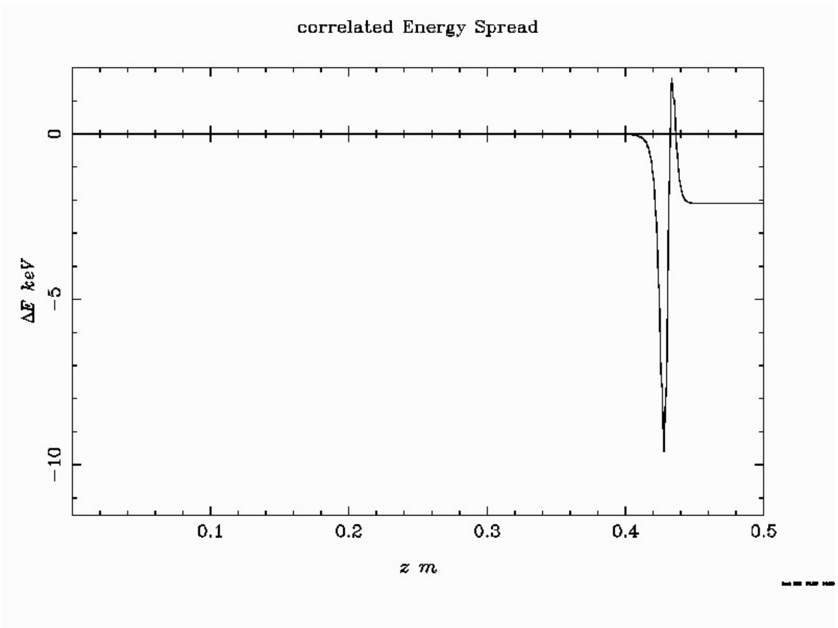

Figure 9: Run 36: Correlated energy spread

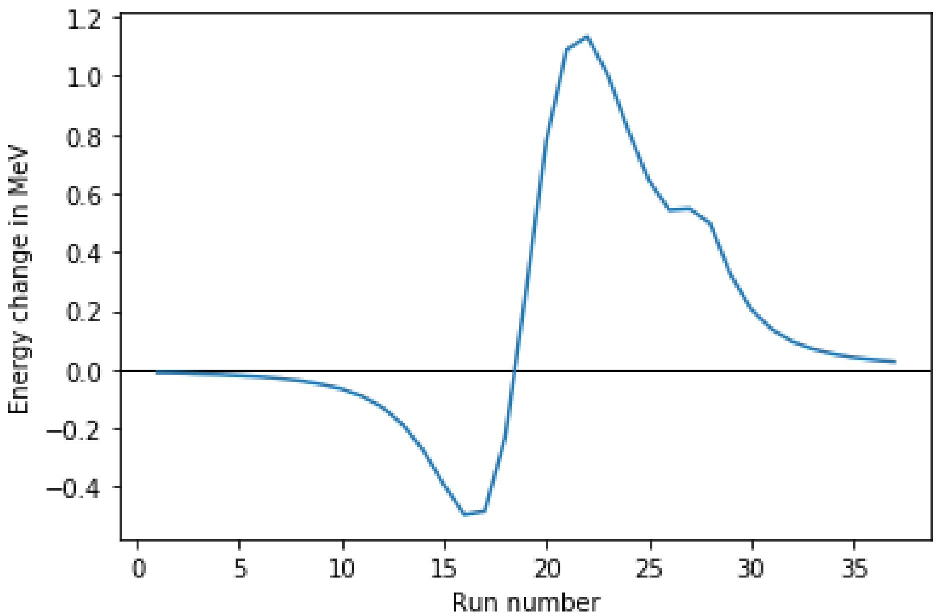

Figure 10: Run 20: Final and initial energy difference vs. the run number. The overtaking point is exactly at the focus ($\Delta z = 0$) somewhere between Run 21 and Run 22

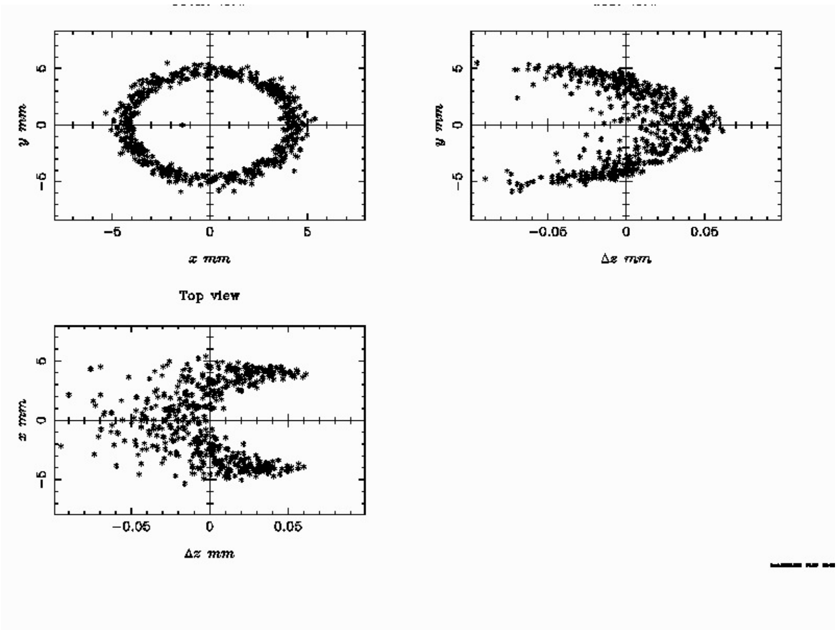

Figure 11: Run 20

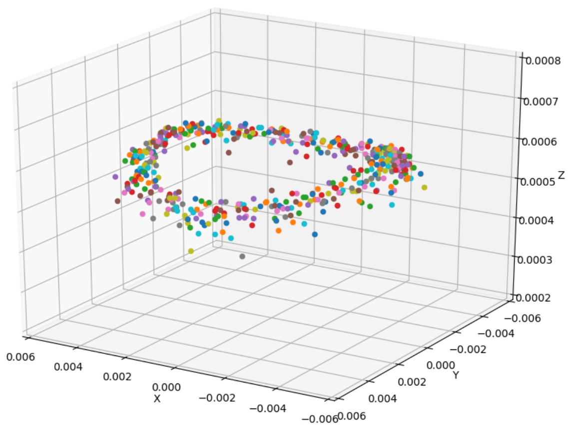

Figure 12: Run 20

(see Fig. 13). On Fig. 13c, it is also clearly seen how the head and the tail of the bunch see different defocusing forces.

The crescents are most likely the result of the laser evolution: the fields, that in a non-evolving wave would have only caused oscillations around a fixed point, could have a net effect due to the intensity change during the overtaking. It is also interesting, that the crescents swap, when the overtaking point is far on the other side of the laser focus (see Fig. 14).

It is important to keep in mind, that the above-shown plots correspond to the longitudinal position $z = 0.5$, which is several centimetres after the end of the interaction. The asymmetry, though, appears earlier.

The "swapping" of the crescents is well visible in Run 25 (Fig. 15), for which $\Delta z \approx 0.007$.

In order to further investigate the case, it is required to decouple the above-described effect from the pure ponderomotive force, which appears due to the pulse shape itself. Reducing the effect of the ponderomotive force would require changing the peak intensity or the pulse shape, which would make the results incomparable with the previous cases. Making the Rayleigh length longer, on the other hand, would significantly reduce the role of the laser evolution, hopefully, without altering the ponderomotive force too much.

Several simulations are done with an increasing beam waist, while a_0 (and, therefore, the peak field in focus) is kept constant. For a higher Rayleigh length the asymmetrical crescents indeed disappear; the particles still form different shapes depending on the energy spread, but these are symmetrical in both planes (Fig. 16).

It is, though, important to make sure that the results are comparable. In Figures 18a and 18b, the behaviour of the divergence and the average energy is shown as the Rayleigh length is being increased. The correlated energy spread changes in an inconsistent way with several peaks (when plotted vs the run number), although it is problematic to compare, as it does not stay constant after the interaction.

On Fig. 17 one can see how the correlated energy spread changes as the Rayleigh length is being increased. Four different Z_R are clearly not enough to analyse the final effect on the bunch, but some tendencies can be already noticed. One can see how the peaks of the curve are sharper and closer to each other for smaller Z_R.

What happens, if the waist increases, but the peak normalised vector potential remains constant? The intensity gradient decreases, but, on the other hand, the beam energy increases and the electron bunch is exposed to comparatively stronger fields. As shown in Fig. 18a, the divergence change is rather small for a big range of Rayleigh lengths. That could mean that the two opposite effects on the transverse ponderomotive force compensate each other. When the Rayleigh length is too high, the divergence falls, as does the final energy; the effects, caused by the laser evolution disappear, as Z_R goes to infinity.

2.5 Asymmetrical effects

Apart from the antisymmetrical effects discussed above, some asymmetry can also be noticed.

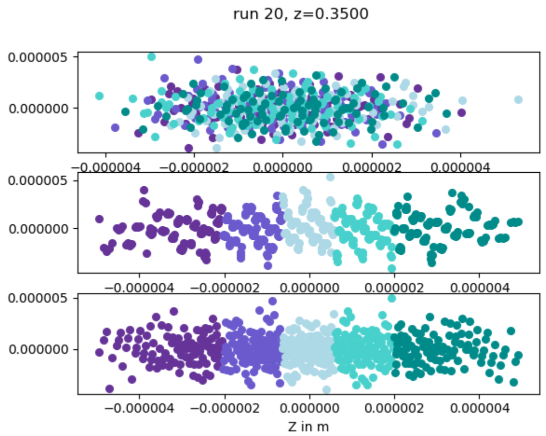

(a)

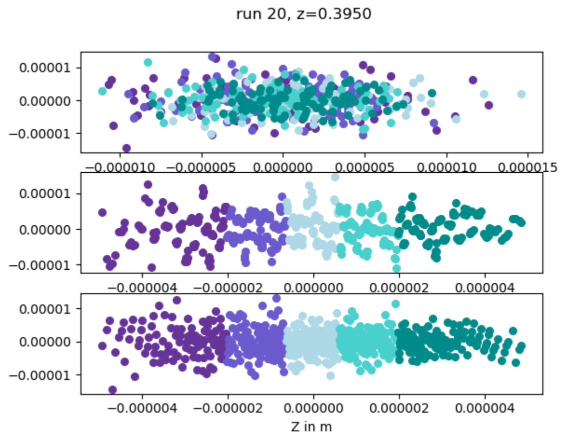

(b)

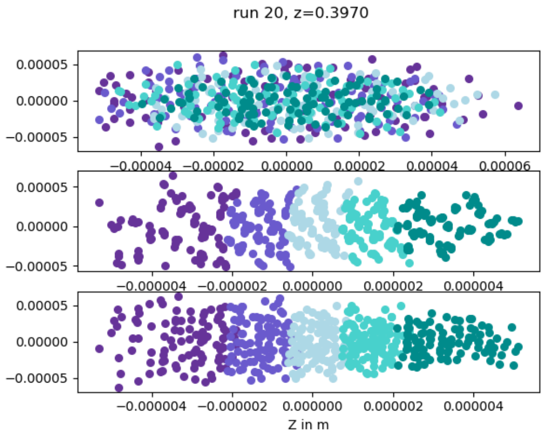

(c)

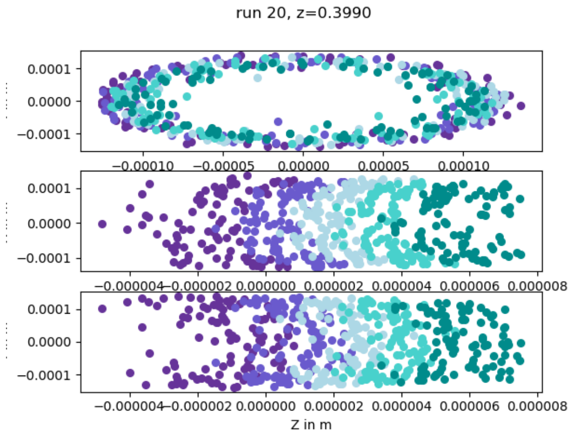

(d)

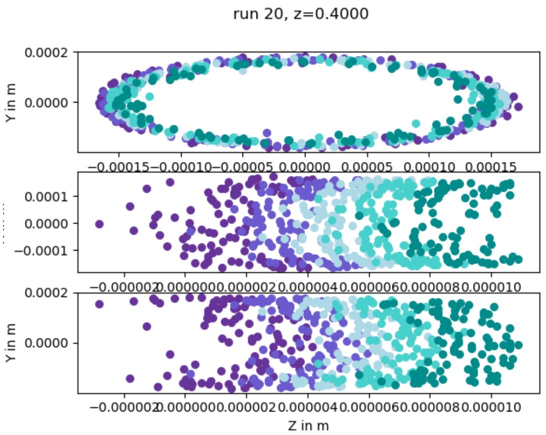

(e)

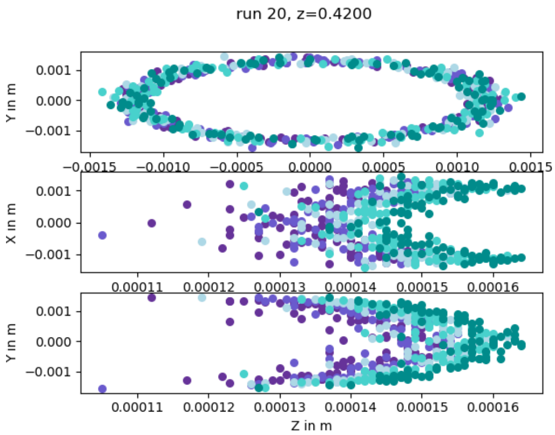

(f)

Figure 13: Run 20: Electron bunch evolution

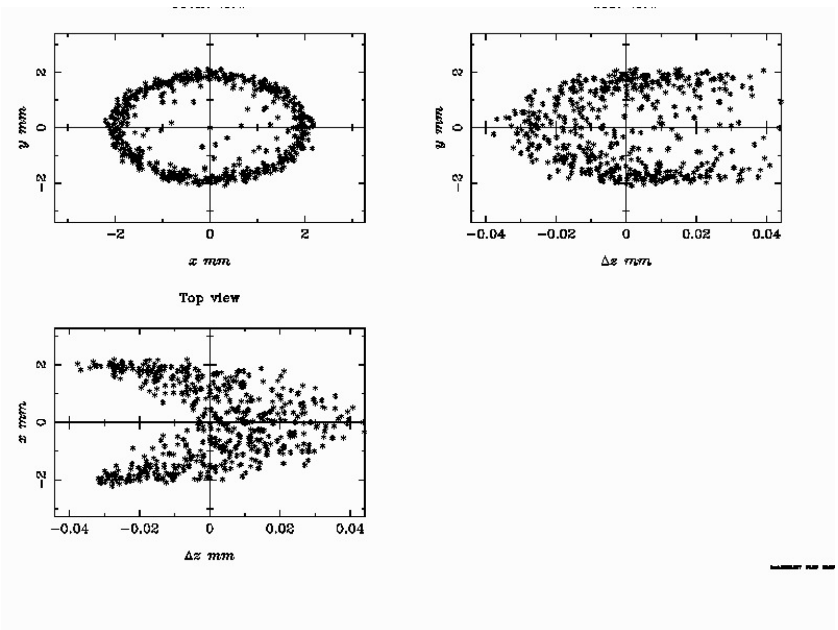

Figure 14: Run 27, $\Delta z_{27} \approx 0.011$: Particle distributions

In all the cases presented in the paragraph "Symmetrical effects", the divergence for x and y is slightly different, the vertical one being higher. Although small, the divergence difference in rather consistent, having a maximum for the Run 25: $\Delta z_{25} \approx 0.007$ (Fig. 19).

The use of the absolute difference instead of a relative one can be justified, as the divergence difference and the divergence itself are caused by different effects.

A corresponding asymmetry is, of course, seen also in the transverse emittance (see, for example, Fig. 5a).

In order to make sure, that it is not a relativistic effect, simulations were run for 3 MeV and 11 MeV, with the peak normalised vector potential scaled down accordingly to have a comparable effect on the transverse emittance. The asymmetry was still present in the both cases, without any significant changes. (As expected, relativity should not break the symmetry.) The comparison for bunches of different energy is, though, problematic, as the overtaking length is different.

To exclude the effects, caused by the longitudinal shape of the bunch, a simulation with a 10 times shorter bunch was done, again, without any significant change in the result.

The asymmetry seems to be linked to the laser evolution, as it decreases with an increasing Rayleigh length, as shown in Fig. 20.

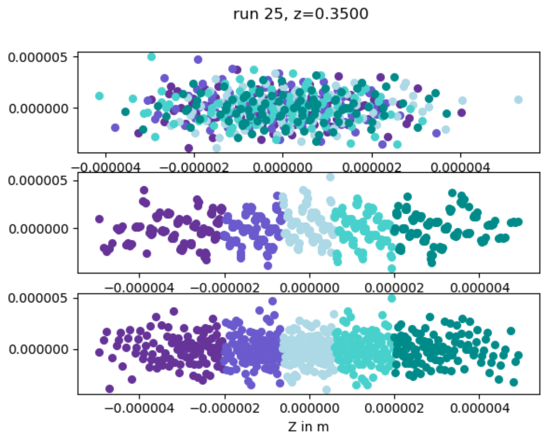

(a)

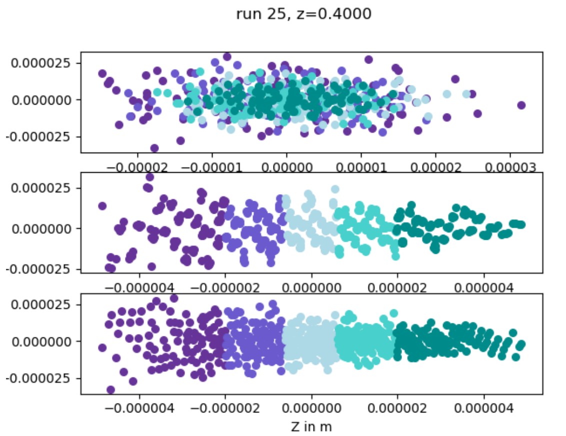

(b)

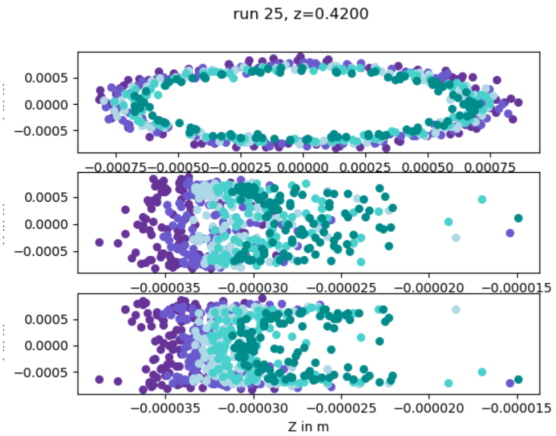

(c)

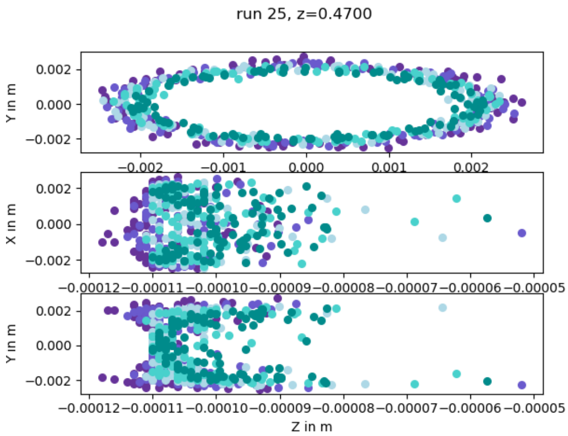

(d)

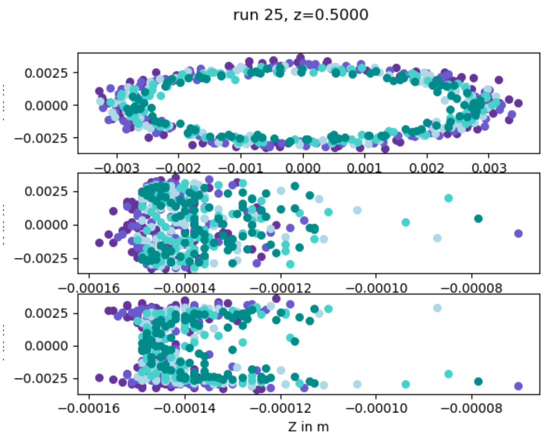

(e)

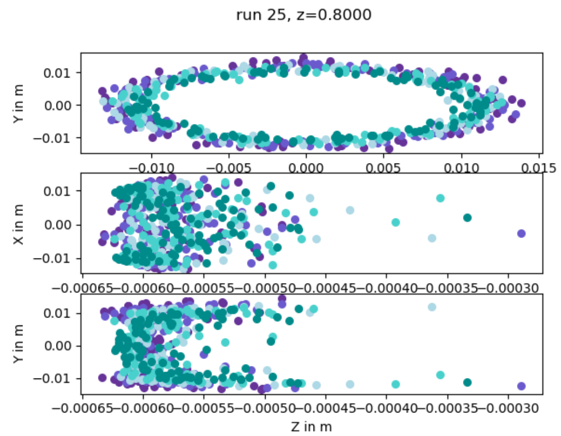

(f)

Figure 15: Run 25: Electron bunch evolution

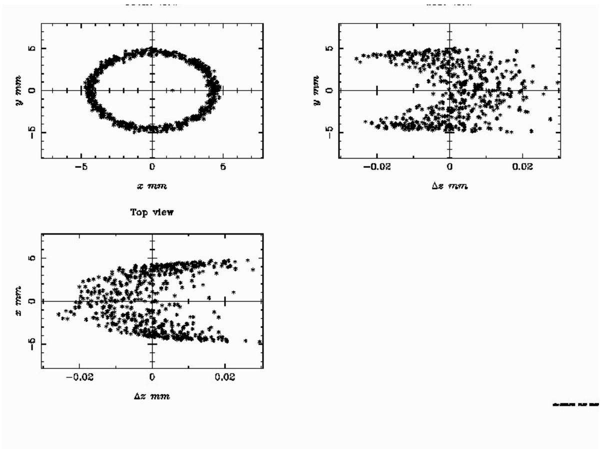

(a) Initial Rayleigh length x4

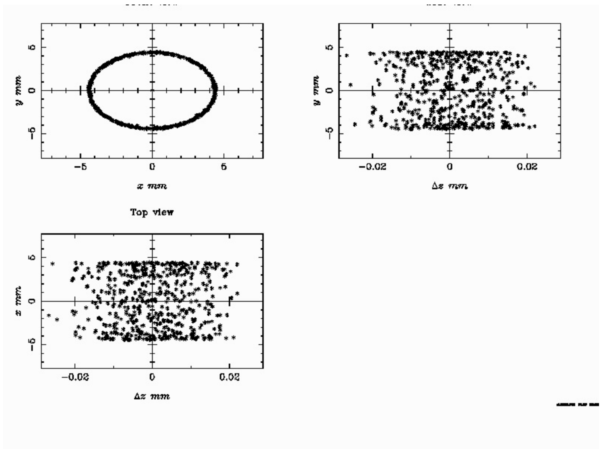

(b) Initial Rayleigh length x32

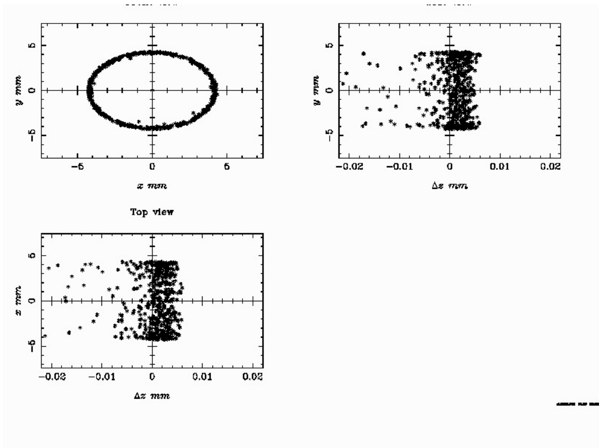

(c) Initial Rayleigh length x64

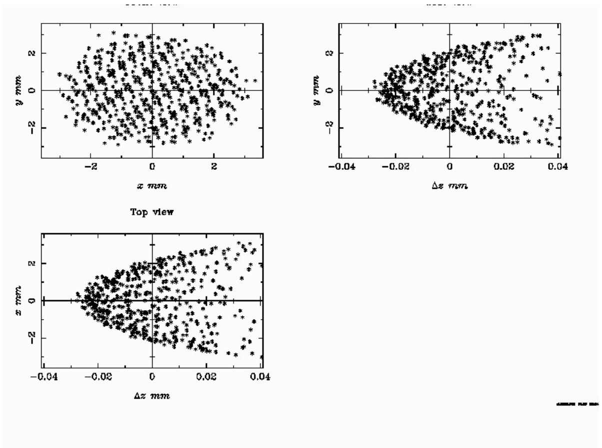

(d) Initial Rayleigh length x128

Figure 16: Run 20: Electron distributions on $z = 0.5$ for different Rayleigh lengths of the laser

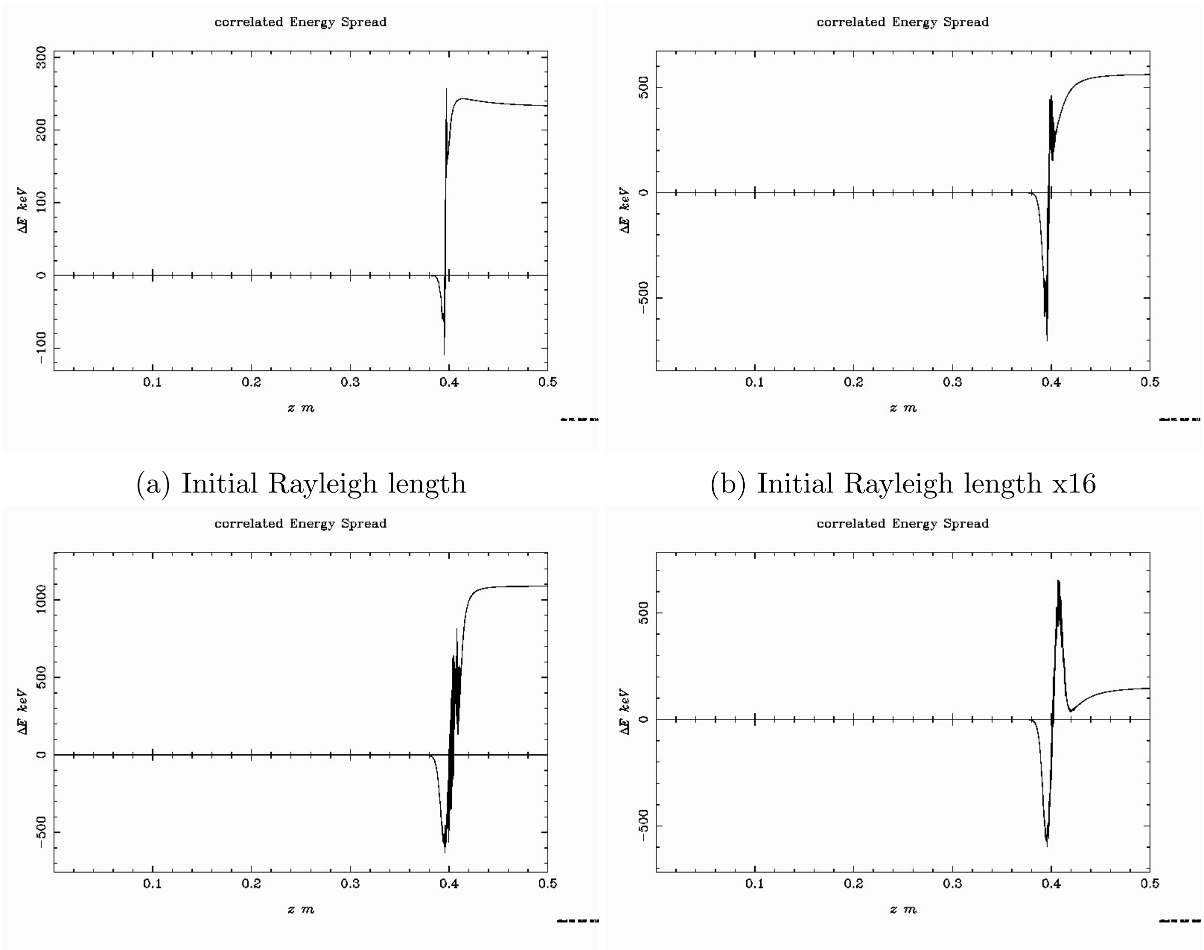

(a) Initial Rayleigh length

(b) Initial Rayleigh length x16

(c) Initial Rayleigh length x64

(d) Initial Rayleigh length x169

Figure 17: Run 20: Correlated energy spread of the bunch for different Rayleigh lengths of the laser

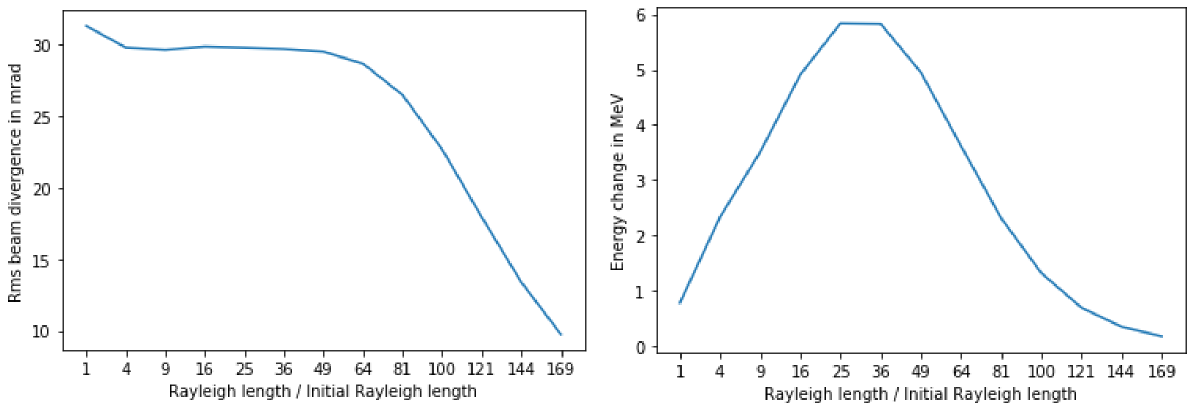

(a) (b)

Figure 18: Run 20: Electron distributions on $z = 0.5$ for different Rayleigh lengths of the laser

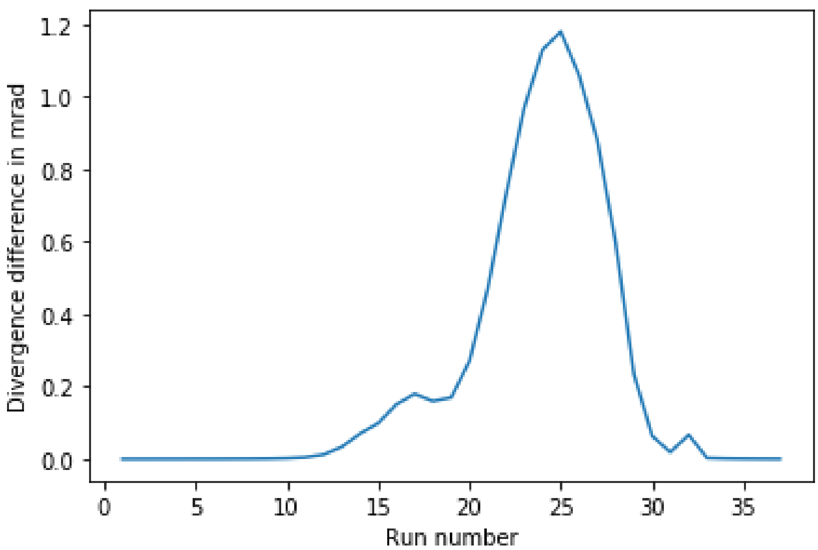

Figure 19: Run 20

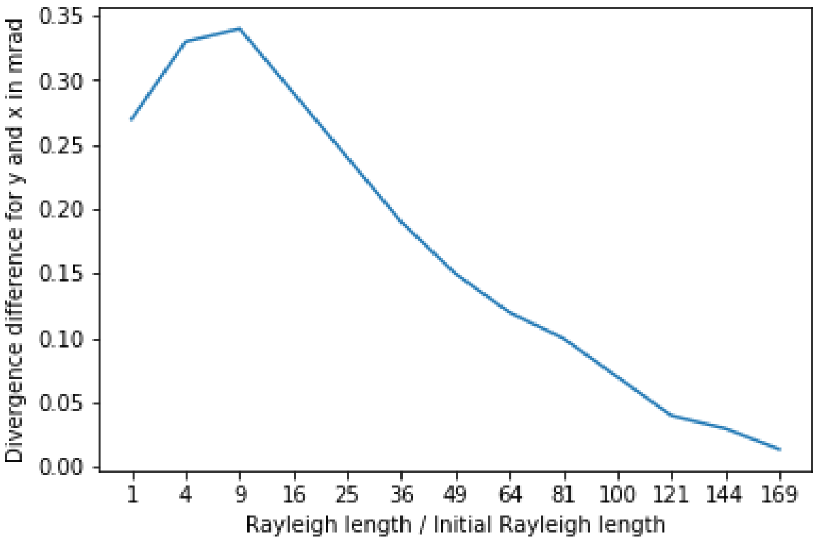

Figure 20: Run 20

3 Conclusion and perspectives

Even in the most basic case presented in the report, the overtaking problem is complex enough due to a number of effects to be considered.

In summary: the bunch parameters are altered due to the ponderomotive force, caused by the pulse shape itself. There are also additional effects coming from the laser evolution, as the field intensity changes during the overtaking. In the end, different parts of the bunch see different fields, so the bunch acquires an energy spread, resulting in peculiar electron distributions.

As a continuation of the work, it would be good to make numerical calculations for higher-order couplings and see if they correspond to the observed asymmetries.

The project was originally conceived as comparison of the overtaking for the cases of Gaussian and Super-Gaussian beams, which is yet to be done. Nevertheless, a deeper study of the Gaussian case and the understanding of the separate effects would make the further analysis for other laser profiles easier.

Acknowledgement

First of all, I would like to thank Klaus Floettmann and Benno Zeitler for giving me this incredible opportunity and for their supervision.

I am grateful to everyone working at REGAE (and beyond) for their patience and immense support during this summer, and for letting me participate in their work.

I would like to express my sincere gratitude to my supervisor Vasilii Tsakanov for introducing me to the field.

Finally, thanks to Benedikt Schmitz and all my friends for the interesting discussions and unforgettable time.

References

[1] B. Zeitler *Phase Space Linearization and External Injection of Electron Bunches into Laser-Driven Plasma Wakefields at REGAE* Ph.D. thesis, University of Hamburg, Hamburg, Germany, 2016

[2] K. Floettmann *ASTRA, a Space Charge Tracking Algorithm,* User Manual, DESY, Hamburg, Germany, 2017

[3] K.T. McDonald *Gaussian Laser Beams with Radial polarisation,* Joseph Henry Laboratories, Princeton University, Princeton, 2000